

Doped holographic fermionic system

Wenjun Huang ^{1,*} Guoyang Fu ^{2,†} Dan Zhang ^{1,‡} Zhenhua Zhou ^{3,§} and Jian-Pin Wu ^{2,¶}

¹ *Department of Physics, School of Mathematics and Physics,*

Bohai University, Jinzhou 121013, China

² *Center for Gravitation and Cosmology,*

College of Physical Science and Technology,

Yangzhou University, Yangzhou 225009, China

³ *School of Physics and Electronic Information,*

Yunnan Normal University, Kunming, 650500, China

Abstract

We numerically construct an AdS black brane geometry with scalar hair, which introduce the doping effect. Over this background, we study the fermionic system with the pseudoscalar Yukawa coupling. This model realize a temperature-doping phase diagram in holographic fermionic system.

^{*}hwj950312@163.com

[†]FuguoyangEDU@163.com

[‡]danzhanglnk@163.com

[§]dtplanck@163.com

[¶]jianpinwu@yzu.edu.cn

I. INTRODUCTION

The holographic duality [1–4] relates a lower-dimensional quantum field theory (QFT) to a classical gravitational system in higher dimensions. It provides us a way to understand strongly-coupled condensed matter systems by constructing a simple gravitational dual model. Also, it can provide some physical insight into the associated mechanisms of these strongly-coupled systems as well as the universality class of them. The well-known examples include the holographic superconductor [5] and (non-) Fermi liquid [6].

Doping plays an essential role in condensed matter system. The temperature-doping phase diagram is landscape of exotic states of matter, including antiferromagnetic (AF) phase, pseudogap phase, strangle metal phase and superconducting phase. How to model the phase diagram and provide a preliminary understanding on it in holography has been an emergent and important topic of research. Some pioneer work have already been devoted to this issue, for example [7, 8]. In these work, they depict the different phases by the properties of the electronic transport.

We can also study this issue by the fermionic response. In holography, we can add probe fermions in the background and study its spectrum. The fermionic spectrum over Reissner-Nordström-AdS (RN-AdS) background exhibits quasi-particle-like excitation around Fermi level, which is non-Fermi liquid [6]. It is consistent with the overall picture of some unconventional phases, such as the normal state of the high- T_c superconducting cuprates, and metals close to a quantum critical point (QCP). Some generalized studies have been widely explored, see [9–21] and therein. Insulating phase can also be implemented in holographic fermionic system by introducing some coupling terms, for example the dipole coupling [22, 23] and pseudoscalar Yukawa coupling [24]. When dipole coupling is introduced, the holographic fermionic system exhibits two key properties of Mott insulating phase, i.e., the emergence of dynamical gap and spectral weight transfer over all energy scale [22, 23]. Lots of studies over more general geometries in [25–41] are implemented, which confirm the robustness of the two key features found in RN-AdS background in [22, 23]. We also observe the emergence of a gap around the Fermi level in the holographic fermionic system with pseudoscalar Yukawa coupling, which indicates an insulating phase [24]. Further studies shows that the insulating phase of the holographic system with pseudoscalar Yukawa coupling is different from the Mott physics [24].

We intend to implement the temperature-doping phase diagram in holographic fermionic system in this paper. To this end, we follow the idea of holographic effective theory to construct a holographic model including two gauge fields and a neutral scalar field. Therefore, we have two independently conserved currents, which relates to different kinds of charge in the dual field theory. The ratio of the two charges plays the role of doping [7]. Over this background, we introduce the pseudoscalar Yukawa coupling as [24] and study its response. This paper is organized as what follows. In Section II, we introduce the holographic framework. Section III presents the numerical results. The conclusion and discussion are presented in Section IV.

II. HOLOGRAPHIC FRAMEWORK

A. Background geometry

We consider the following action

$$S = \frac{1}{2\kappa^2} \int d^4x \sqrt{-g} \left(R + \frac{6}{L^2} + \mathcal{L}_M + \mathcal{L}_\Phi \right), \quad (1)$$

where \mathcal{L}_M and \mathcal{L}_Φ are given in what follows,

$$\mathcal{L}_M = -\frac{1}{4}Z_A(\Phi)F_{\mu\nu}F^{\mu\nu} - \frac{1}{4}Z_B(\Phi)G_{\mu\nu}G^{\mu\nu} - \frac{1}{2}Z_{AB}(\Phi)F_{\mu\nu}G^{\mu\nu}, \quad (2a)$$

$$\mathcal{L}_\Phi = -\frac{1}{2}\nabla_\mu\Phi\nabla_\nu\Phi - \frac{1}{2}m^2\Phi^2. \quad (2b)$$

We choose the specific forms of the coupling function $Z_A(\Phi)$, $Z_B(\Phi)$ and $Z_{AB}(\Phi)$ as

$$Z_A(\Phi) = 1 + \frac{1}{2}\alpha\Phi^2, \quad Z_B(\Phi) = 1 + \frac{1}{2}\beta\Phi^2, \quad Z_{AB}(\Phi) = \frac{1}{2}\gamma\Phi^2. \quad (3)$$

This theory includes two gauge fields A and B and the corresponding field strengths are $F = dA$ and $G = dB$, respectively. Φ is a neutral scalar field, which has the dimension Δ relating to the mass of the scalar field as $m^2L^2 = \Delta(\Delta - 3)$.

The equations of motion (EOMs) can be straightforward derived from the action (1) as

$$R_{\mu\nu} - \left(\frac{1}{2}R + \frac{3}{L^2} \right)g_{\mu\nu} + \frac{1}{2}(T_{\mu\nu}^A + T_{\mu\nu}^\Phi) = 0, \quad (4a)$$

$$\nabla_\mu (Z_A(\Phi)F^{\mu\nu} + Z_{AB}(\Phi)G^{\mu\nu}) = 0, \quad (4b)$$

$$\nabla_\mu (Z_B(\Phi)G^{\mu\nu} + Z_{AB}(\Phi)F^{\mu\nu}) = 0, \quad (4c)$$

$$\left(\nabla^2 - m^2 - \left(\frac{1}{4}\alpha F^2 + \frac{1}{4}\beta G^2 + \frac{1}{2}\gamma F_{\mu\nu}G^{\mu\nu} \right) \right) \Phi = 0, \quad (4d)$$

where

$$T_{\mu\nu}^A = -\mathcal{L}_M g_{\mu\nu} - Z_A(\Phi) F_{\mu\rho} F_{\nu}^{\rho} - Z_B(\Phi) G_{\mu\rho} G_{\nu}^{\rho} - 2Z_{AB}(\Phi) F_{(\mu|\rho|} G_{\nu)}^{\rho}, \quad (5a)$$

$$T_{\mu\nu}^{\Phi} = -\mathcal{L}_{\Phi} g_{\mu\nu} - \nabla_{\mu} \Phi \nabla_{\nu} \Phi. \quad (5b)$$

The symmetry bracket in $T_{\mu\nu}^A$ means $A_{(\mu\nu)} = (A_{\mu\nu} + A_{\nu\mu})/2$.

We shall numerically construct the black brane solution with non-trivial scalar profile. We assume the following ansatz¹

$$ds^2 = \frac{1}{u^2} \left[-(1-u)pU dt^2 + \frac{du^2}{(1-u)pU} + Vdx^2 + Vdy^2 \right], \quad (6a)$$

$$A = \mu(1-u)adt, \quad (6b)$$

$$B = \delta\mu(1-u)bdt, \quad (6c)$$

$$\Phi = u^{3-\Delta}\phi, \quad (6d)$$

where $p(u) = 1 + u + u^2 - \mu^2 u^3/4$. μ and $\delta\mu$ are the chemical potentials of the dual boundary field theory of the gauge fields A and B . These two controllable chemical potentials or charge densities induce the unbalance of numbers². The ration $\chi = \frac{\delta\mu}{\mu}$ represents the amount of charged impurities, which is introduced to simulate the doping [7].

U , V , a and b are the function of the radial coordinate u only. The temperature of the dual boundary field theory is

$$\hat{T} = \frac{(12 - \mu^2)U(1)}{16\pi}. \quad (7)$$

And then we can define a scaling-invariant temperature $T \equiv \hat{T}/\mu$. To support an asymptotic AdS black bran, we set the boundary conditions as $U(0) = V(0) = a(0) = b(0) = 1$ at the UV boundary. It is easy to derive the asymptotic behavior of $\phi(u)$ at UV boundary, which follows

$$\phi(u) = \phi_0 + \phi_1 u^{2\Delta-3}. \quad (8)$$

We identify ϕ_0 and ϕ_1 as the source and expectation, respectively. The source ϕ_0 corresponds to the coupling of the boundary QFT and deforms it.

¹ Here and in what follows, we shall set $L = 1$.

² Two gauge fields are introduced to simulate unbalanced mixtures in holography, which can be found in [42–47] and therein. In addition, in [48], two gauge fields are also introduced to study metal insulator phase transition.

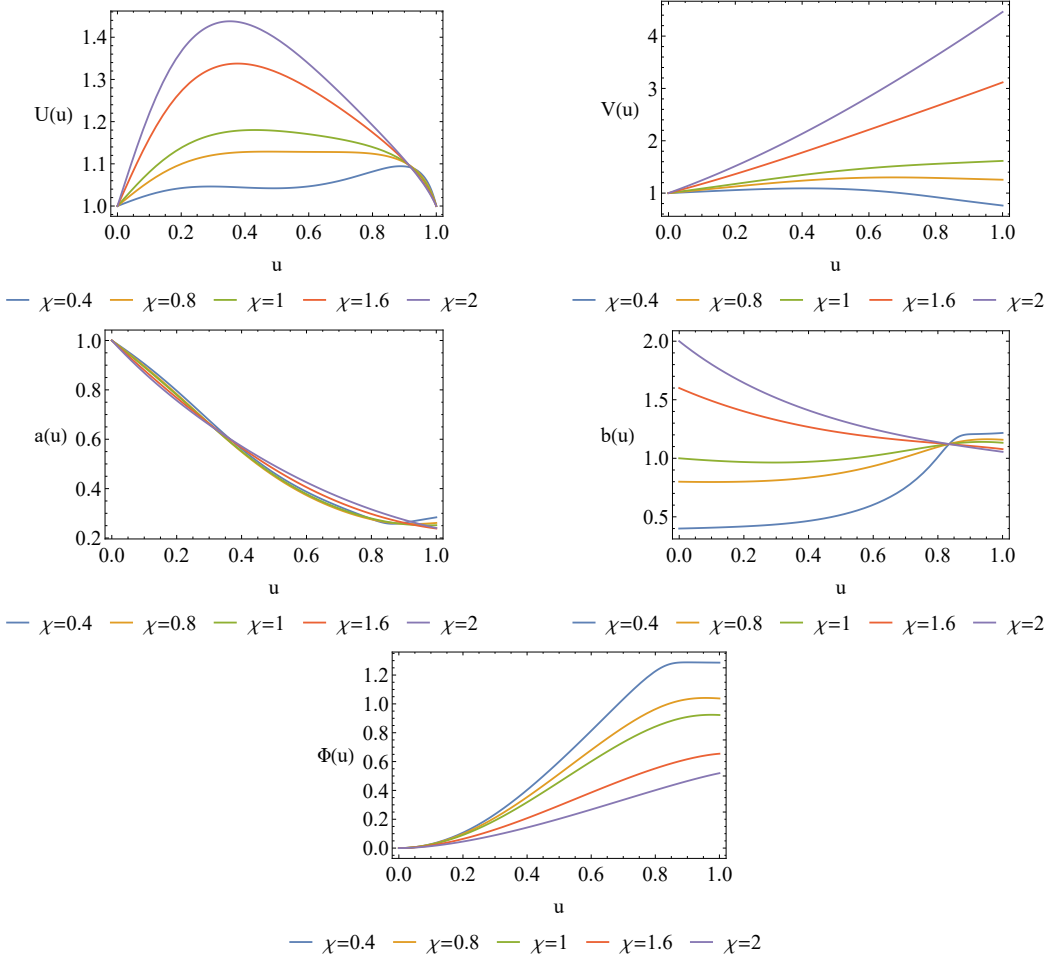


FIG. 1: Plots of $U(u)$, $V(u)$, $a(u)$, $b(u)$ and $\Phi(u)$ as the function of u with different doping χ at $T = 0.01$.

For given scalar field mass m^2 and the coupling parameters α , β and γ , the system is determined by three scaling-invariant parameters, namely, the Hawking temperature T , the doping χ and the coupling $\lambda \equiv \phi_0/\mu^{3-\Delta}$. We mainly focus on the effect of the doping, so we turn off ϕ_0 , i.e., setting $\phi_0 = 0$. In addition, we fix the parameters as $\alpha = 5$, $\beta = -1$, $\gamma = 1$ and $\Delta = 2$ through this paper.

To numerically solve the EOMs, we need to impose the boundary conditions at the UV boundary and the horizon. At the UV boundary, $u \rightarrow 0$, we require that the geometry approaches AdS_4 with deformations corresponding to chemical potential μ and ϕ follows the behavior of Eq. (8). At the horizon, $u \rightarrow 1$, the regular boundary conditions should be imposed. FIG.1 shows the plots of $U(u)$, $V(u)$, $a(u)$, $b(u)$ and $\Phi(u)$ as the function of u with different doping χ at $T = 0.01$. Some brief comments, which is helpful to understand

the picture of the fermionic spectrum studied in following section, are summarized as what follows.

- With the increase of χ , the value of $\Phi(u)$ decreases at the horizon but vanishes near the UV boundary. It is a crucial ingredient in understanding the pseudoscalar coupling effect because the pseudoscalar coupling provides a direct coupling between scalar field and Dirac field.
- The value of the metric $V(u)$ increases at the horizon as χ increases.
- When we tune χ , the gauge field χ greatly changes whether at the horizon or near the UV boundary. Especially, the change is very evident near the UV boundary.

B. Dirac equation

To study the fermionic spectrum, we consider the following Dirac action with Yukawa coupling between the spinor field and the scalar field over this gravitational background [24]

$$S_D = i \int d^4x \sqrt{-g\zeta} (\Gamma^a \mathcal{D}_a - m_\zeta) \zeta, \quad (9a)$$

$$S_Y = \int d^4x \sqrt{-g} [\eta_2 \bar{\zeta} \Phi \Gamma^5 \zeta + h.c.] . \quad (9b)$$

$\Gamma^a = (e_\mu)^a \Gamma^\mu$ with $(e_\mu)^a$ being a set of orthogonal normal vector bases. $\mathcal{D}_a = \partial_a + \frac{1}{4}(\omega_{\mu\nu})_a \Gamma^{\mu\nu} - iqA_a$ where $(\omega_{\mu\nu})_a$ is the spin connection 1-forms. Γ^5 is the chirality matrix, which satisfies $\{\Gamma^5, \Gamma^\mu\} = 0$.

From the above actions (9a) and (9b), we have the following Dirac equation

$$\Gamma^a \mathcal{D}_a \zeta - m_\zeta \zeta - i\eta_2 \Phi \Gamma^5 \zeta = 0. \quad (10)$$

In order to numerically solve the Dirac equation and read off the fermionic spectrum, we make a redefinition of $\zeta = (g_{tt}g_{xx}g_{yy})^{-\frac{1}{4}} \mathcal{F}$ and expand \mathcal{F} in momentum space as

$$\mathcal{F} = \int \frac{d\omega dk}{2\pi} F(u, k) e^{-i\omega t + ikx}, \quad (11)$$

where we have set $k_x = k$ and $k_y = 0$. In addition, we split the spinor into $F = (F_1, F_2)^T$ with $F_\alpha \equiv (\mathcal{A}_\alpha, \mathcal{B}_\alpha)^T$, $\alpha = 1, 2$, and choose a specific gamma matrices as

$$\Gamma^3 = \begin{pmatrix} -\sigma^3 & 0 \\ 0 & -\sigma^3 \end{pmatrix}, \quad \Gamma^0 = \begin{pmatrix} i\sigma^1 & 0 \\ 0 & i\sigma^1 \end{pmatrix}, \quad \Gamma^1 = \begin{pmatrix} -\sigma^2 & 0 \\ 0 & \sigma^2 \end{pmatrix},$$

$$\Gamma^2 = \begin{pmatrix} 0 & \sigma^2 \\ \sigma^2 & 0 \end{pmatrix}, \quad \Gamma^5 = \begin{pmatrix} 0 & i\sigma^2 \\ -i\sigma^2 & 0 \end{pmatrix}. \quad (12)$$

And then, we have the following Dirac equation of 4-component spinor

$$\left(\frac{1}{\sqrt{g_{uu}}} \partial_u \mp m_\zeta \right) \begin{pmatrix} \mathcal{A}_1 \\ \mathcal{B}_1 \end{pmatrix} \pm (\omega + qA_t) \frac{1}{\sqrt{g_{tt}}} \begin{pmatrix} \mathcal{B}_1 \\ \mathcal{A}_1 \end{pmatrix} - \frac{k}{\sqrt{g_{xx}}} \begin{pmatrix} \mathcal{B}_1 \\ \mathcal{A}_1 \end{pmatrix} + i\eta_2 \Phi \begin{pmatrix} \mathcal{B}_2 \\ \mathcal{A}_2 \end{pmatrix} = 0, \quad (13)$$

$$\left(\frac{1}{\sqrt{g_{uu}}} \partial_u \mp m_\zeta \right) \begin{pmatrix} \mathcal{A}_2 \\ \mathcal{B}_2 \end{pmatrix} \pm (\omega + qA_t) \frac{1}{\sqrt{g_{tt}}} \begin{pmatrix} \mathcal{B}_2 \\ \mathcal{A}_2 \end{pmatrix} + \frac{k}{\sqrt{g_{xx}}} \begin{pmatrix} \mathcal{B}_2 \\ \mathcal{A}_2 \end{pmatrix} - i\eta_2 \Phi \begin{pmatrix} \mathcal{B}_1 \\ \mathcal{A}_1 \end{pmatrix} = 0. \quad (14)$$

In order to solve the above Dirac equation, we impose the following boundary at the horizon [24]

$$\begin{pmatrix} \mathcal{A}_\alpha(u, \mathbf{k}) \\ \mathcal{B}_\alpha(u, \mathbf{k}) \end{pmatrix} = c_\alpha \begin{pmatrix} 1 \\ -i \end{pmatrix} (1-u)^{-\frac{i\omega}{4\pi T}}. \quad (15)$$

Near the AdS boundary, the behavior of the Dirac field follows

$$\begin{pmatrix} \mathcal{A}_\alpha \\ \mathcal{B}_\alpha \end{pmatrix} \approx a_\alpha u^{m_\zeta} \begin{pmatrix} 1 \\ 0 \end{pmatrix} + b_\alpha u^{-m_\zeta} \begin{pmatrix} 0 \\ 1 \end{pmatrix}. \quad (16)$$

By holography, we can read off the retarded Green function

$$a_\alpha = G_{\alpha\alpha'} b_{\alpha'}. \quad (17)$$

And then, we shall study the measurable spectral function $A(\omega, k_x, k_y) \sim \text{Im}(\text{Tr}G)$.

III. NUMERICAL RESULTS

In this section, we shall study this holographic fermionic system by numerically solving the Dirac equations (13) and (14). Note that in this paper, we only focus on the case of $m_\zeta = 0$. FIG.2 show the density plots of spectral function $A(\omega, k)$ for $\chi = 1$ at $T = 0.01$ (left panel is for $\eta_2 = 0$ and right panel for $\eta_2 = 4$). When $\eta_2 = 0$, a small bump emerges near the Fermi level ($\omega = 0$). It is different from that over RN-AdS background for which a sharp peak shows up near $\omega = 0$ [6]. When we turn down the doping parameter χ , the

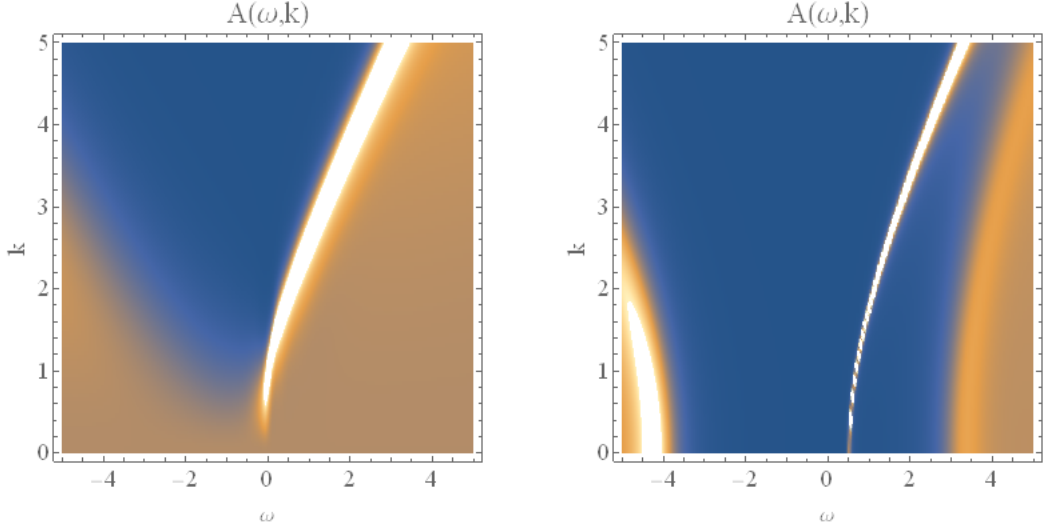


FIG. 2: Density plots of spectral function $A(\omega, k)$ for $\chi = 1$ at $T = 0.01$. Left plot is for $\eta_2 = 0$ and right plot for $\eta_2 = 4$.

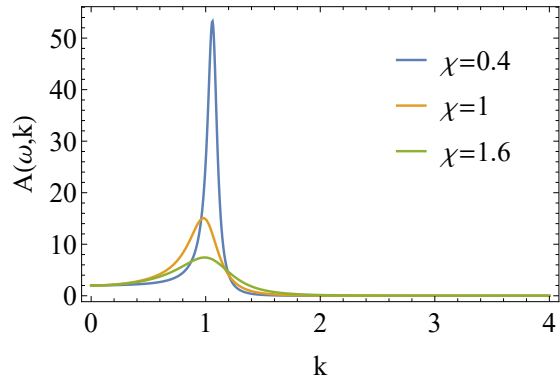


FIG. 3: Spectral function $A(\omega, k)$ for $\eta_2 = 0$ and different χ at $T = 0.01$.

bump becomes a small peak (FIG.3). Conversely, when we turn up χ , the bump becomes smaller (FIG.3). It indicates that the doping suppresses the bump at Fermi level.

When we turn on the pseudoscalar Yukawa coupling η_2 and tune it large, we find that a gap emerges around $\omega = 0$ when η_2 is beyond some critical value (right panel in FIG.2). FIG.4 further shows the process of the emergence of the gap. From FIG.4, we clearly see that for $\eta_2 = 0$, the peaks (bumps) distribute near $\omega = 0$. While for $\eta_2 = 4$, the peaks (bumps) disappears around $\omega = 0$ and a gap emerges around $\omega = 0$ instead. In particular, with the increase of k , the peaks (bumps) are pushed away from $\omega = 0$, which confirms that the gap exists for all k .

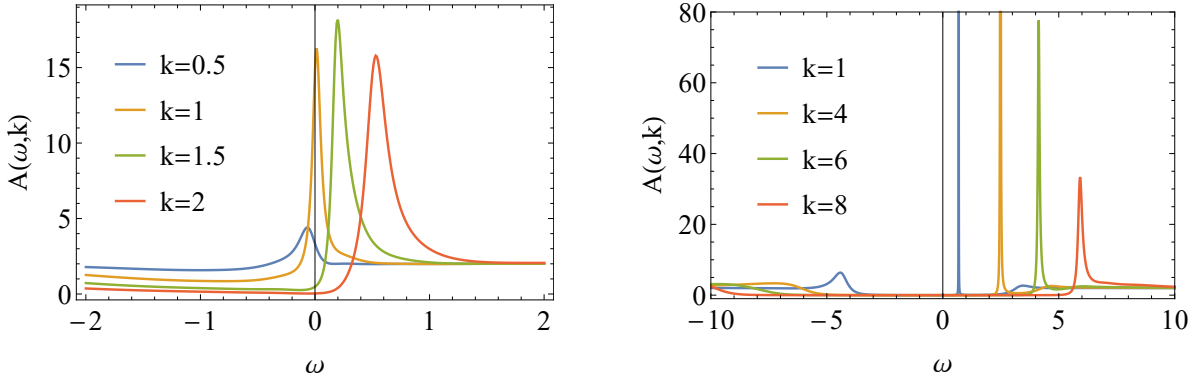


FIG. 4: Spectral function $A(\omega, k)$ with $\chi = 1$ at $T = 0.01$ for sample k . Left plot is for $\eta_2 = 0$ and right plot for $\eta_2 = 4$.

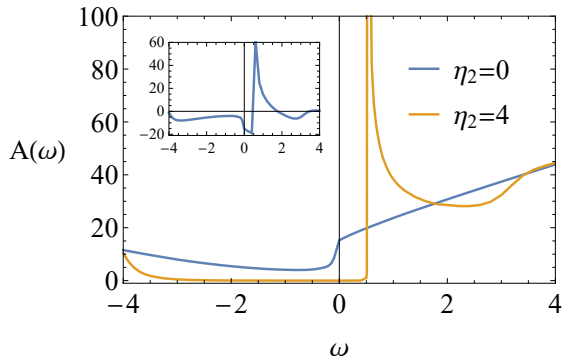


FIG. 5: DOS $A(\omega)$ as the function of ω for different η_2 . Here $\chi = 1$ and $T = 0.01$. The inset shows $A(\omega, \eta_2 = 4) - A(\omega, \eta_2 = 0)$ as a function of ω .

The density of state (DOS) is an effective measure to study the properties of the gap. It is defined as the integral of the spectral function $A(\omega, k)$ over k space and measures the total weight of the spectral function. FIG.5 shows DOS $A(\omega)$ as the function of ω for different η_2 . We summarize the properties as what follows.

- The spectrum rearranges at low frequency region (the absolute value $|\omega|$ is small), which is induced by the pseudoscalar Yukawa coupling. It attributes to the non-trivial profile of scalar field near horizon.
- As η_2 increases, there is the transfer of the spectral weight from the low energy band ($\omega < 0$) to the high energy band ($\omega > 0$). The transfer is over low energy scales but not over all energy scales. It is different from the Mott physics and also that in RN-AdS background, for which the spectral weight transfers over all energy scales. From

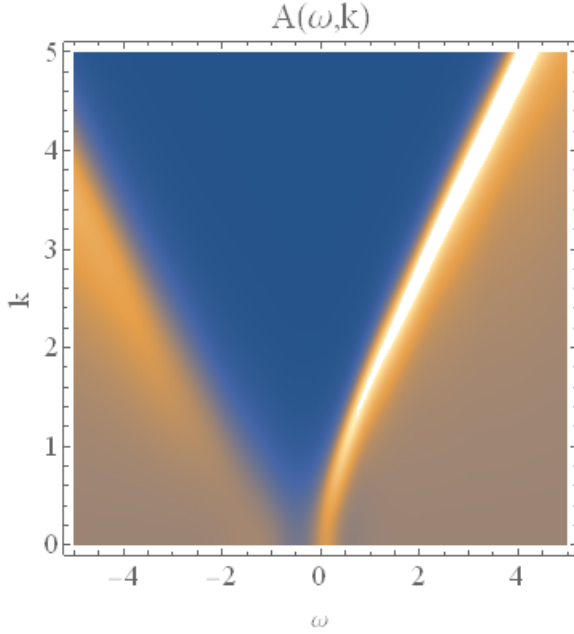


FIG. 6: The density plot of spectral function $A(\omega, k)$ for $\chi = 1$ and $\eta_2 = 4$ at $T = 0.15$.

FIG.5, especially the inset of FIG.5 which exhibits the difference between $A(\omega, \eta_2 = 4)$ and $A(\omega, \eta_2 = 0)$, we see that when $|\omega|$ is large (the high frequency region), the DOS for all η_2 approaches the same value. It is because the scalar field vanishes on the UV boundary.

These properties are the same as that revealed in [24]. Therefore, we conclude that even when the doping is introduced in this system, it do not change the basic properties from pseudoscalar Yukawa coupling.

When we heat this fermionic system with doping, we find that the gap closes (see FIG.6). It is a universal property shared by Mott physics, the fermionic system with dipole coupling [22, 23], and also that from pseudoscalar Yukawa coupling [24].

Now, we turn to quantitatively study the effect from the doping. To this end, we introduce the critical value of the onset of the gap η_2^c to signal the formation of the gap. It is identified as that the DOS at the Fermi level drops below some small number. In numerical calculation, we take this number as 10^{-3} . Left plot in FIG.7 and TABLE I show the relation between the doping χ and η_2^c . The study indicates that when the doping becomes large, the gap emerges more difficult. Note that with the increase of χ , the amplitude of the scalar field near the horizon become more evident (see FIG.1 and the associated comments in section II A),

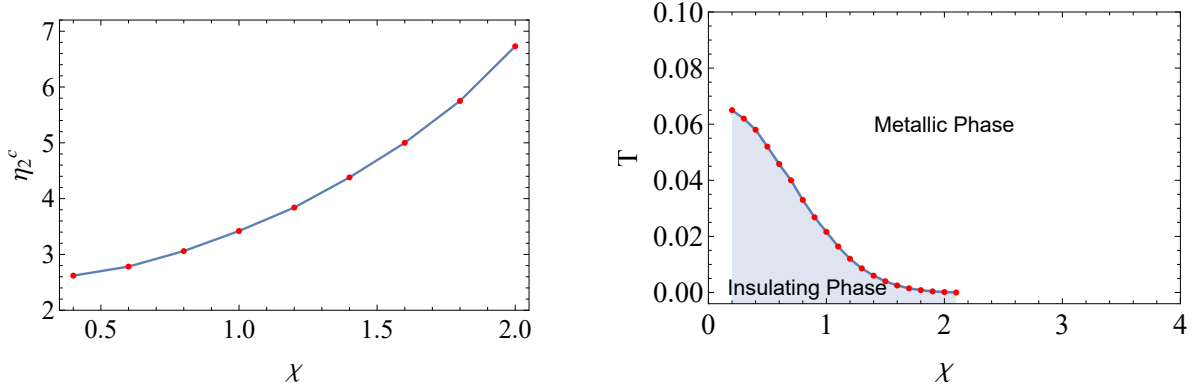


FIG. 7: Left plot: The relation between the doping χ and η_2^c at $T = 0.01$. Right plot: Phase diagram (χ, T) of the model. Here we have fixed the pseudoscalar Yukawa coupling $\eta_2 = 4$.

which usually make the gap open more easily as observed in [24] because the low frequency spectrum probes the near horizon geometry. But here we observe a contrary result. It indicates that there is a competition between the pseudoscalar Yukawa coupling and the doping. The essential reason may be from the background geometry and in particular the profiles of the gauge field B , which are greatly changed by the doping (see FIG.1). But deeper understanding on this issue, we need to implement an analytical study. We leave it for future work.

χ	0.4	0.8	1	1.6	2
η_2^c	2.620	3.06	3.420	5.000	6.730

TABLE I: η_2^c with different χ at $T = 0.01$.

Now, we fix the pseudoscalar Yukawa coupling to explore the temperature-doping phase diagram (χ, T) . Right plot in FIG.7 shows phase diagram (χ, T) . Here we have fixed the pseudoscalar Yukawa coupling $\eta_2 = 4$. From this figure, we can see that when both the temperature and the doping are low, an insulating phase emerges. For fixed temperature, with the increase of the doping, there is a phase transition from insulating phase to metallic phase. Especially, due to the introduction of doping parameter, we can easily tune the temperature approaching to zero. Therefore, a QCP can be implemented in our model. But we would also like to point out that when the doping parameter is small (being approximately lower than the value of $\chi = 0.35$ in our present model), it is difficult to find the background solution. Therefore, we can not obtain a compact insulating region around the origin of the

(χ, T) plane. We hope to improve our model to realize this case in future study. In short, when the doping is introduced, it implements the temperature-doping phase diagram (χ, T) in holographic fermionic system. Therefore, it can provide us a platform to study richer physics in future, in particular model the phase diagram of some materials.

IV. CONCLUSION AND DISCUSSION

In this paper, we introduce a two-current model, which includes two gauge fields and a neutral scalar field, which support an AdS black brane geometry with scalar hair. This model introduces two tuneable chemical potentials, which induce unbalance of numbers and so introduce a controllable doping parameter. The study on the fermionic response shows that with the increase of the doping, the gap opens more difficult. This result indicates that there is a competition between the pseudoscalar Yukawa coupling and the doping. It attributes to greatly change of the background geometry and the profiles of the gauge fields as well as scalar field causing by the doping. An important result of this paper is to exhibit the temperature-doping phase diagram in holographic fermionic system. It helps to further reproduce real phase diagram of some materials in holographic fermionic system and explore some universal properties of holographic system in future.

Lots of topics deserve further exploration. One immediate topic is to introduce the momentum dissipation such that we can the temperature-doping phase diagram in terms of both the electric transport and the fermionic response. In particular, it is important to study the consistent picture from the the electric transport and the fermionic response.

Acknowledgments

This work is supported by the Natural Science Foundation of China under Grant Nos. 11775036, 11905182. J. P. Wu is also supported by Top Talent Support Program from Yangzhou University.

[1] J. M. Maldacena, “The Large N limit of superconformal field theories and supergravity,” *Adv. Theor. Math. Phys.* **2**, 231 (1998) [hep-th/9711200].

- [2] S. S. Gubser, I. R. Klebanov and A. M. Polyakov, “Gauge theory correlators from noncritical string theory,” *Phys. Lett. B* **428**, 105 (1998) [hep-th/9802109].
- [3] E. Witten, “Anti-de Sitter space and holography,” *Adv. Theor. Math. Phys.* **2**, 253 (1998) [hep-th/9802150].
- [4] O. Aharony, S. S. Gubser, J. M. Maldacena, H. Ooguri and Y. Oz, “Large N field theories, string theory and gravity,” *Phys. Rept.* **323**, 183 (2000) [hep-th/9905111].
- [5] S. A. Hartnoll, C. P. Herzog and G. T. Horowitz, “Building a Holographic Superconductor,” *Phys. Rev. Lett.* **101** (2008) 031601. [arXiv:0803.3295 [hep-th]].
- [6] H. Liu, J. McGreevy and D. Vegh, “Non-Fermi liquids from holography,” *Phys. Rev. D* **83**, 065029 (2011) [arXiv:0903.2477 [hep-th]].
- [7] E. Kiritsis and L. Li, “Holographic Competition of Phases and Superconductivity,” *JHEP* **1601**, 147 (2016) [arXiv:1510.00020 [cond-mat.str-el]].
- [8] M. Baggioli and M. Goykhman, “Under The Dome: Doped holographic superconductors with broken translational symmetry,” *JHEP* **1601**, 011 (2016) [arXiv:1510.06363 [hep-th]].
- [9] J. P. Wu, “Holographic fermions in charged Gauss-Bonnet black hole,” *JHEP* **1107**, 106 (2011) [arXiv:1103.3982 [hep-th]].
- [10] Y. Liu, K. Schalm, Y. W. Sun and J. Zaanen, “Lattice Potentials and Fermions in Holographic non Fermi-Liquids: Hybridizing Local Quantum Criticality,” *JHEP* **1210**, 036 (2012) [arXiv:1205.5227 [hep-th]].
- [11] Y. Ling, C. Niu, J. P. Wu, Z. Y. Xian and H. b. Zhang, “Holographic Fermionic Liquid with Lattices,” *JHEP* **1307**, 045 (2013) [arXiv:1304.2128 [hep-th]].
- [12] J. P. Wu, “Some properties of the holographic fermions in an extremal charged dilatonic black hole,” *Phys. Rev. D* **84**, 064008 (2011) [arXiv:1108.6134 [hep-th]].
- [13] U. Gursoy, E. Plauschinn, H. Stoof and S. Vandoren, “Holography and ARPES Sum-Rules,” *JHEP* **1205**, 018 (2012) [arXiv:1112.5074 [hep-th]].
- [14] M. Alishahiha, M. R. Mohammadi Mozaffar and A. Mollabashi, “Fermions on Lifshitz Background,” *Phys. Rev. D* **86**, 026002 (2012) [arXiv:1201.1764 [hep-th]].
- [15] L. Q. Fang, X. H. Ge and X. M. Kuang, “Holographic fermions in charged Lifshitz theory,” *Phys. Rev. D* **86**, 105037 (2012) [arXiv:1201.3832 [hep-th]].
- [16] W. J. Li and J. P. Wu, “Holographic fermions in charged dilaton black branes,” *Nucl. Phys. B* **867**, 810 (2013) [arXiv:1203.0674 [hep-th]].

- [17] J. Wang, “Schrodinger Fermi liquids,” *Phys. Rev. D* **89**, no. 4, 046008 (2014) [arXiv:1301.1986 [hep-th]].
- [18] J. P. Wu, “Holographic fermions on a charged Lifshitz background from Einstein-Dilaton-Maxwell model,” *JHEP* **1303**, 083 (2013).
- [19] X. M. Kuang, E. Papantonopoulos, B. Wang and J. P. Wu, “Formation of Fermi surfaces and the appearance of liquid phases in holographic theories with hyperscaling violation,” *JHEP* **1411**, 086 (2014) [arXiv:1409.2945 [hep-th]].
- [20] L. Q. Fang, X. H. Ge, J. P. Wu and H. Q. Leng, “Anisotropic Fermi surface from holography,” *Phys. Rev. D* **91**, no. 12, 126009 (2015) [arXiv:1409.6062 [hep-th]].
- [21] L. Q. Fang and X. M. Kuang, “Holographic Fermions in Anisotropic Einstein-Maxwell-Dilaton-Axion Theory,” *Adv. High Energy Phys.* **2015**, 658607 (2015).
- [22] M. Edalati, R. G. Leigh and P. W. Phillips, “Dynamically Generated Mott Gap from Holography,” *Phys. Rev. Lett.* **106**, 091602 (2011) [arXiv:1010.3238 [hep-th]].
- [23] M. Edalati, R. G. Leigh, K. W. Lo and P. W. Phillips, “Dynamical Gap and Cuprate-like Physics from Holography,” *Phys. Rev. D* **83**, 046012 (2011) [arXiv:1012.3751 [hep-th]].
- [24] J. P. Wu, “Dynamical gap driven by Yukawa coupling in holography,” *Eur. Phys. J. C* **79**, no. 8, 691 (2019).
- [25] J. P. Wu and H. B. Zeng, “Dynamic gap from holographic fermions in charged dilaton black branes,” *JHEP* **1204**, 068 (2012) [arXiv:1201.2485 [hep-th]].
- [26] X. M. Kuang, B. Wang and J. P. Wu, “Dipole Coupling Effect of Holographic Fermion in the Background of Charged Gauss-Bonnet AdS Black Hole,” *JHEP* **1207**, 125 (2012) [arXiv:1205.6674 [hep-th]].
- [27] W. Y. Wen and S. Y. Wu, “Dipole Coupling Effect of Holographic Fermion in Charged Dilatonic Gravity,” *Phys. Lett. B* **712**, 266 (2012) [arXiv:1202.6539 [hep-th]].
- [28] X. M. Kuang, B. Wang and J. P. Wu, “Dynamical gap from holography in the charged dilaton black hole,” *Class. Quant. Grav.* **30**, 145011 (2013) [arXiv:1210.5735 [hep-th]].
- [29] J. P. Wu, “Emergence of gap from holographic fermions on charged Lifshitz background,” *JHEP* **1304**, 073 (2013).
- [30] J. P. Wu, “The charged Lifshitz black brane geometry and the bulk dipole coupling,” *Phys. Lett. B* **728**, 450 (2014).
- [31] X. M. Kuang, E. Papantonopoulos, B. Wang and J. P. Wu, “Dynamically generated gap from

holography in the charged black brane with hyperscaling violation,” JHEP **1504**, 137 (2015) [arXiv:1411.5627 [hep-th]].

[32] Y. Ling, P. Liu, C. Niu, J. P. Wu and Z. Y. Xian, “Holographic fermionic system with dipole coupling on Q-lattice,” JHEP **1412**, 149 (2014) [arXiv:1410.7323 [hep-th]].

[33] G. Vanacore, P. W. Phillips, “Minding the Gap in Holographic Models of Interacting Fermions,” Phys. Rev. D **90**, 044022 (2014) [arXiv:1405.1041 [cond-mat.str-el]].

[34] Z. Fan, “Dynamic Mott gap from holographic fermions in geometries with hyperscaling violation,” JHEP **1308**, 119 (2013) [arXiv:1305.1151 [hep-th]].

[35] L. Q. Fang, X. M. Kuang, B. Wang and J. P. Wu, “Fermionic phase transition induced by the effective impurity in holography,” JHEP **1511**, 134 (2015) [arXiv:1507.03121 [hep-th]].

[36] J. P. Wu, “Holographic fermionic spectrum from Born-Infeld AdS black hole,” Phys. Lett. B **758**, 440 (2016) [arXiv:1705.06707 [hep-th]].

[37] X. M. Kuang and J. P. Wu, “Effect of quintessence on holographic fermionic spectrum,” Eur. Phys. J. C **77**, no. 10, 670 (2017).

[38] L. Q. Fang, X. M. Kuang and J. P. Wu, “The holographic fermions dual to massive gravity,” Sci. China Phys. Mech. Astron. **59**, no. 10, 100411 (2016).

[39] L. Q. Fang, X. H. Ge and X. M. Kuang, “Holographic fermions with running chemical potential and dipole coupling,” Nucl. Phys. B **877**, 807 (2013) [arXiv:1304.7431 [hep-th]].

[40] Y. Ling, P. Liu, C. Niu and J. P. Wu, “Pseudo-gap phase and duality in a holographic fermionic system with dipole coupling on Q-lattice,” Chin. Phys. C **40**, no. 4, 043102 (2016) [arXiv:1602.06062 [hep-th]].

[41] Y. Seo, G. Song, Y. H. Qi and S. J. Sin, “Mott transition with Holographic Spectral function,” arXiv:1803.01864 [hep-th].

[42] J. Erdmenger, V. Grass, P. Kerner and T. H. Ngo, “Holographic Superfluidity in Imbalanced Mixtures,” JHEP **1108**, 037 (2011) [arXiv:1103.4145 [hep-th]].

[43] F. Bigazzi, A. L. Cotrone, D. Musso, N. Pinzani Fokeeva and D. Seminara, “Unbalanced Holographic Superconductors and Spintronics,” JHEP **1202**, 078 (2012) [arXiv:1111.6601 [hep-th]].

[44] D. Musso, “Competition/Enhancement of Two Probe Order Parameters in the Unbalanced Holographic Superconductor,” JHEP **1306**, 083 (2013) [arXiv:1302.7205 [hep-th]].

[45] A. Amoretti, A. Braggio, N. Maggiore, N. Magnoli and D. Musso, “Coexistence of two vector order parameters: a holographic model for ferromagnetic superconductivity,” JHEP **1401**,

054 (2014) [arXiv:1309.5093 [hep-th]].

[46] J. Alsup, E. Papantonopoulos and G. Siopsis, “FFLO States in Holographic Superconductors,” arXiv:1208.4582 [hep-th].

[47] J. Alsup, E. Papantonopoulos and G. Siopsis, “A Novel Mechanism to Generate FFLO States in Holographic Superconductors,” *Phys. Lett. B* **720**, 379 (2013) [arXiv:1210.1541 [hep-th]].

[48] Y. Ling, P. Liu and J. P. Wu, “A novel insulator by holographic Q-lattices,” *JHEP* **1602**, 075 (2016) [arXiv:1510.05456 [hep-th]].